

DOI:10.1002/ejic.201402153

Thermochromic and Piezochromic Effects of Co^{II}-Imidazole-Based Supramolecular Gels as Logic Gates

Sung Ho Jung,^[a] Jong Hun Moon,^[b] Jin Yong Lee,^{*[b]} and Jong Hwa Jung^{*[a]}

Keywords: Gels / N ligands / Logic gate / Supramolecular chemistry / Cobalt

We demonstrate that the imidazole-based ligand **1** efficiently produces a coordination polymer gel by simple mixing with Co²⁺ ion. When the molar ratio of CoCl₂ to ligand **1** was less < 1, a red sol was obtained, indicating the formation of an octahedral (O_h) complex species as occurs with Co(NO₃)₂. In contrast to **G1**, when the amount of CoCl₂ employed was more than 1 equiv., the color of the gel changed from red to blue (**G2**), indicating the formation of mainly a tetrahedral

(T_d) complex species. The ionochromic and the piezochromic effects of imidazole-based supramolecular gel with Co²⁺ were investigated. These effects of supramolecular gel were controlled by various anions of cobalt, which are due to coordination geometric change of gels. Interestingly, the ionochromic and piezochromic effects of **G1** act as AND and OR logic gates in the solid and the gel state.

Introduction

Coordination polymer gels of metal–organic frameworks (MOFs) obtained by self-assembly of metal ions and multi-functional ligands have attracted considerable attention not only because of their many unique structural features, but also because of their various potential applications, which include gas storage, separation, catalysis, and sensor technology.^[1] Metal–organic complexes with specific thermochromic properties have heretofore been used as thermochromic materials.

Thermochromism in metal–organic complexes is usually the result of a solid-to-solid phase transition, which may result from changes in the coordination geometry around the metal center, including a change in the coordination number.^[2] It is useful to study such materials to help understand the various factors that influence the color change. Among the transition-metal ions, Co²⁺ is a classical example that shows chromism upon ligand exchange (often induced by a temperature change) in the solid and gel states, as is commonly observed in the hydration-induced color change of indicating silica gel.^[3] For example, Kimizuka et al.^[4] reported the thermochromic properties of Co²⁺

complexes with triazole-based ligands in the gel state upon changing the temperature. In the presence of Co²⁺, the triazole-based ligand formed a blue coordination polymer gel in which the metal atom had a tetrahedral structure at high temperature. At low temperature, the triazole-based ligand did not form a gel but yielded an octahedral complex structure, which was red. At intermediate temperatures, tetrahedral and octahedral Co²⁺ species coexisted. However, the different chromic properties and exact coordination geometries of the Co²⁺ coordination polymer gels under various external stimuli such as the concentrations of the metal ion and anion present, the pressure, and the temperature have been less studied. As far as we know, only three examples of such studies have been reported.^[5,6] However, the influence on the coordination geometries of Co²⁺ complexes in the gel state have not been systematically studied by the application of external stimuli such as the presence of anions, heating, and mechanical grinding.

With this objective in the mind, we investigated changes in the coordination geometry of a Co²⁺ supramolecular gel that occurred in the presence of different anions. In particular, we were successful in probing the coordination geometry in the supramolecular gel by single-crystal X-ray analysis and computer simulations. As an extension of this study, the Co²⁺ supramolecular gels were used as soft and solid logic gates.

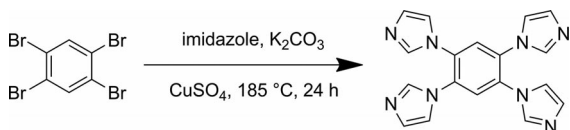
Results and Discussion

Tetraimidazole-based ligand **1** was synthesized according to a literature method (Scheme 1).^[7] The incorporation of the central benzene moiety in **1** gave rise to 2D network structures in the resulting supramolecular assemblies.

[a] Department of Chemistry and Research Institute of Natural Sciences Gyeongsang National University, Jinju 660-701, Korea
E-mail: jonghwa@gnu.ac.kr
www.nanochem.campushomepage.com

[b] Department of Chemistry and Institute of Basic Science Sungkyunkwan University, Suwon 440-746, Korea
E-mail: jinylee@skku.edu
http://home.skku.edu/~jinylee/

Supporting information for this article is available on the WWW under <http://dx.doi.org/10.1002/ejic.201402153>.



Scheme 1. Synthetic route to ligand **1**.

For the preparation of the self-assembled coordination polymer gel, 1,2,4,5-tetrakis(1-imidazolyl)benzene (**1**) was dissolved in a chosen organic solvent, and Co^{2+} (0.5–3.0 equiv.) was dissolved in the same solvent. This Co^{2+} solution was then added to the solution of **1** without heating. The molar ratio of the metal ion with respect to **1** (2.0 wt.-%) ranged from 0.5 to 3.0, corresponding to a molar ratio of the gelator to the solvent of approximately $1:10^4$. Compound **1** immediately formed a gel upon the addition of Co^{2+} with a variety of cobalt anions such as ClO_4^- , Cl^- , Br^- , I^- , and NO_3^- (Figure 1a) in the polar solvents DMF, dimethylacetamide (DMA), and DMF/ H_2O (1:1, v/v) upon mixing the solutions. Except for solutions containing Cl^- and Br^- , these gels were reddish in color (Figure 1a). From these results, we concluded that the formation of a Co^{2+} coordination polymer gel with **1** did not strongly depend on the nature of the anion. Figure 1b shows a field-emission scanning electron microscopy (FE-SEM) image of coordination polymer gel **1** with $\text{Co}(\text{NO}_3)_2$. The fiber structure has a diameter of 50–100 nm. In addition, SEM images of the coordination polymer gels obtained by using different anions showed fiber structures with diameters in the 50–150 nm range (Figure S1, Supporting Information). Thus, the nature of the anion had little influence on the morphology of Co^{2+} gel **1**.

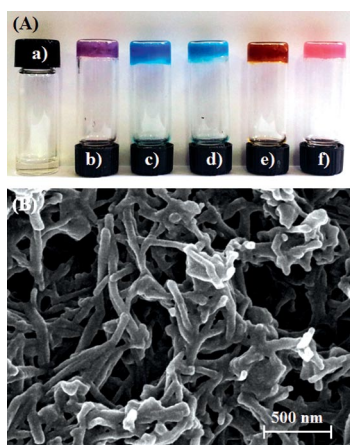


Figure 1. (A) Photographs of Co^{2+} coordination polymer gels **1** (2.0 wt.-%) (a) without a metal ion and with (b) $\text{Co}(\text{ClO}_4)_2$, (c) CoCl_2 , (d) CoBr_2 , (e) CoI_2 , and (f) $\text{Co}(\text{NO}_3)_2$ (3.0 equiv.) in DMF. (B) SEM image of coordination polymer gel **1** (2.0 wt.-%) with $\text{Co}(\text{NO}_3)_2$ (3.0 equiv.).

The UV/Vis absorption spectra of gel **1** obtained from $\text{Co}(\text{NO}_3)_2$ and CoCl_2 in DMF are shown in Figure 2. The UV/Vis spectrum of $\text{Co}(\text{NO}_3)_2$ gel **1** (i.e., **G1**) exhibited an absorption maximum at 518 nm, corresponding to a red

color (Figure 2A) and suggested the formation of octahedral (O_h) coordination. If **G1** was heated to above 100°C , the absorption intensity of the O_h complex was slightly weakened, and the gelation was destroyed. No significant change in the red color occurred, which indicated that **G1** maintained its octahedral structure. In contrast, if the molar ratio of CoCl_2 to ligand **1** was less than 1 (Figure 2B; Figure S2, Supporting Information), a red sol was obtained, which indicated that the formation of an O_h complex species occurred with $\text{Co}(\text{NO}_3)_2$ (Figure 2B). In contrast to **G1**, if the amount of CoCl_2 employed was more than 1 equiv., the color of the gel changed from red to blue (i.e., **G2**; Figure S2, Supporting Information). The UV/Vis spectra of **G2** at various molar ratios (0.5, 0.7, 0.9, 1.0, 2.0, and 3.0) exhibited an absorption maximum at 680 nm [T_d , ${}^4A_2 \rightarrow {}^4T_1(\text{P})$] for the blue species, and this is characteristic of a tetrahedral Co^{2+} . The absorption intensity at the 680 nm band of **G2** gradually increased as the mol ratio of CoCl_2 was increased, and a maximum was reached at a mol ratio > 3.0 . The O_h complex of sol **1** with CoCl_2 was converted into the T_d complex, and it turned into a gel. The T_d complex coexists with the O_h complex in the gel phase. To calculate the O_h complex component, the extinction coefficient for **1b** with the octahedral structure was calculated. Then, the component of the octahedral structure in the absorption band of **G2** was analyzed by the curve-fitting method. A considerable fraction of the O_h complex (ca. 20%) was present at a mol ratio of 2.0. The octahedral structure of **1** with CoCl_2 is favored in solution, whereas the tetrahedral structure is favored in the gel state. This outcome may be caused by the coordination bonding strength.

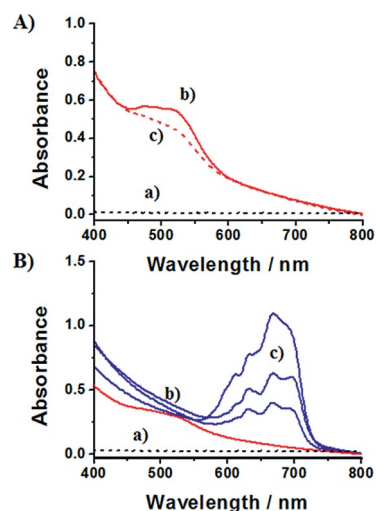


Figure 2. (A) UV/Vis spectra of (a) **1** (1.0 mm) in DMF and (b) **G1** (2.0 wt.-%, $\text{Co}(\text{NO}_3)_2$: 3.0 equiv.) in DMF. (B) UV/Vis spectra of (a) **1** (1.0 mm), (b) sol **1** (CoCl_2 : 0.5 equiv.) in DMF, and (c–e) **G2** (CoCl_2 : 1.0, 2.0, and 3.0 equiv.) in DMF.

We observed a color change of **G1** obtained from **1** with $\text{Co}(\text{NO}_3)_2$ upon the addition of other anions. The red color of **G1** changed to blue upon the addition of a small amount

of a solution containing Cl^- or Br^- ions (Figure S3, Supporting Information). As mentioned already, such a color change reflects a change in **G1** from an O_h structure to a T_d structure, a phenomenon termed the ionochromic effect.^[8] More interestingly, the red color of dry **G1** changed to blue if a mixture of the former and KBr powder was mechanically ground, and this behavior is referred to as the piezochromic effect.^[9] In contrast, no significant color changes were observed upon the addition of F^- , I^- , SO_4^{2-} , or CH_3COO^- .

To further elucidate the driving forces for gel formation as well as the relationship between the color differences and the geometries of **G1** and **G2**, we attempted to grow X-ray quality red and blue single crystals of the corresponding Co^{2+} complexes of **1** from the gel phase. However, the red single crystal obtained from **1** with $\text{Co}(\text{NO}_3)_2$ was not high enough in quality for X-ray crystallographic analysis. Therefore, we optimized the most stable structure of **1** with $\text{Co}(\text{NO}_3)_2$ by using DFT calculations.^[10] The optimized structure of the complex of **1** with $\text{Co}(\text{NO}_3)_2$ for **1a** is shown in Figure 3. For **1a**, the optimized structure revealed a 2D coordination polymer network of formula $\{[\text{Co}_2(\mathbf{1})_2(\text{NO}_3)_2(\text{H}_2\text{O})_2] \cdot (\text{NO}_3)_2(\text{H}_2\text{O})_2\}_n$. Interestingly, the two Co atoms (Co1 and Co2), which bridge **1**, have different coordination environments (Figure S4a, Supporting Information). The Co1 atom located at the inversion center is hexacoordinate, and it is bonded to four different nitrogen atoms from **1** in a monodentate manner. The octahedral coordination sphere was completed by two additional water molecules. The Co2 atom is bonded to four nitrogen atoms from different molecules of **1** in a monodentate manner. The octahedral coordination sphere is completed by two monodentate nitrates. The Co1–N distances (2.072 and 2.139 Å) are longer than the Co1–O(water) (2.037 Å) distances. The Co2–N distances (2.052 and 2.075 Å) are shorter than the Co2–O(NO_3^-) (2.156 Å) distances (Table S1, Supporting Information). Hence, gel formation by **G1** likely reflects the formation of a network structure involving coordination bonding between Co^{2+} and the nitrogen atoms of ligand **1**.

In contrast, the red color of a single crystal in the complex of **1** with CoCl_2 was retained in DMF solution. For red **1b**, structure determination revealed a 2D coordination polymer of formula $[\text{Co}(\mathbf{1})\text{Cl}_2]_n$ (**1b**; Figure S4b, Supporting Information). The asymmetric unit of **1b** consists of one quarter of **1**, one quarter of a Co atom, and one half of two Cl^- . The Co^{2+} center is also octahedrally coordinated to four nitrogen atoms from a different bridging molecule of **1** and two Cl^- anions. The Co1–N distance (2.129 Å) is shorter than the Co1–Cl1(Cl^-) distance (2.522 Å; Tables S2 and S3, Supporting Information). However, the bond between Co^{2+} and Cl^- is longer than that between Co^{2+} and NO_3^- . Given that the blue single crystal obtained from **G2** was too poor in quality to allow single-crystal X-ray determination, we investigated the coordination geometry of **G2** by using computer simulations.

We also investigated color changes of single crystals of initially red **1a** and **1b** by optical microscopy by means of

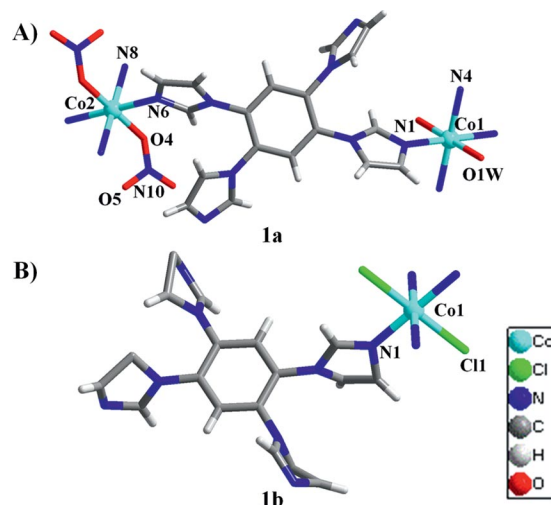


Figure 3. (A) Optimized structure of the complex of **1** with $\text{Co}(\text{NO}_3)_2$ in the gel state. (B) Single-crystal structure of the complexes of **1** derived from CoCl_2 obtained from the sol state.

a heated stage. As shown in Figure 4, single-crystal **1a** maintained its red color up to 200 °C, in accord with the fact that the O_h complex of **G1** with $\text{Co}(\text{NO}_3)_2$ is quite stable. In contrast, a single crystal of **1b** changed partially from red to blue at 100 °C and changed completely to blue at 140 °C. This color-change behavior is quite different from that observed for a single crystal of **1a** obtained from **G1**. The O_h complex of **1b** obtained from **1** with CoCl_2 changed into a T_d complex, because this complex is less stable than that of **1a**. The color changes of **1b** are due to the bonding strength between Co and Cl^- , which is weaker than that obtained between Co and NO_3^- . The results are in agreement with a single-crystal X-ray study.

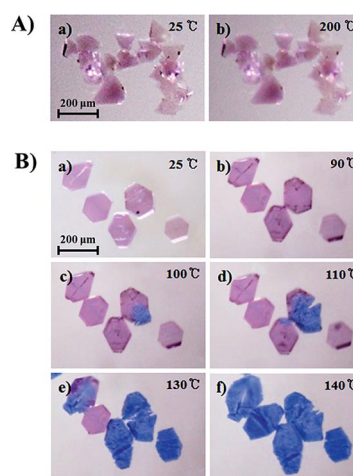


Figure 4. Color changes upon heating (A) **1a** and (B) **1b** obtained by optical microscopy.

To investigate the different thermal stability of single crystals of the Co^{2+} complexes with respect to temperature, we calculated the relative binding free energy of the

$\text{CoCl}_2(\mathbf{1})_n$ ($n = 2$ and 4) complex of $\mathbf{1b}$ obtained from complexation of $\mathbf{1}$ with CoCl_2 and that of the $\text{Co}_2(\mathbf{1})_2(\text{NO}_3)_2(\text{H}_2\text{O})_2$ complex of $\mathbf{1a}$ by using DFT calculations (Figure 5A; Figure S5, Supporting Information). As shown in Figure 5, the binding free energies of three- and four-coordinate $[\text{CoCl}_2(\mathbf{1})]$ and $[\text{CoCl}_2(\mathbf{1})_2]$; $\mathbf{1c}$ were negative in the temperature range from 370 to 420 K, whereas those of the penta- and hexacoordinate $[\text{CoCl}_2(\mathbf{1})_3]$ and $[\text{CoCl}_2(\mathbf{1})_4]$ complexes were positive. This result is consistent with the experimental observation that $\mathbf{1b}$ changes into $\mathbf{1c}$ upon heating.

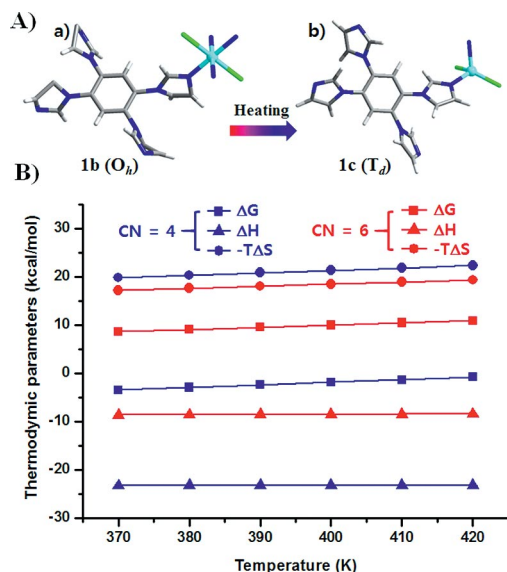


Figure 5. (A, a) Single-crystal structure of the complex of $\mathbf{1}$ with CoCl_2 ($\mathbf{1b}$). (A, b) Optimized tetrahedral structure of the complex of $\mathbf{1}$ with CoCl_2 ($\mathbf{1c}$) obtained by DFT calculations. (B) Temperature dependence of the enthalpy (ΔH), entropy ($-T\Delta S$), and free energy (ΔG) change of $\text{CoCl}_2(\mathbf{1})_{n-1} + \mathbf{1} \rightarrow \text{CoCl}_2(\mathbf{1})_n$. [CN (coordination number) = $4/6$ for $n = 2/4$].

We further investigated the enthalpy and entropy changes for $\text{CoCl}_2(\mathbf{1})_n$ ($n = 2, 3, 4$) as representative cases. As seen in Figure 5B, the enthalpy was negative for both $n = 2$ (ca. $-24 \text{ kcal mol}^{-1}$) and $n = 4$ (ca. $-10 \text{ kcal mol}^{-1}$); however, the entropy contribution ($-T\Delta S$) was positive (ca. 20 kcal mol^{-1}). This tendency was also observed for $n = 3$. Thus, the $\text{CoCl}_2(\mathbf{1})_n \rightarrow \text{CoCl}_2(\mathbf{1})_{n-1} + \mathbf{1}$ reaction would be spontaneous, which is consistent with the experiment.

From the calculated free energy of the T_d complex ($\mathbf{1c}$: -4.43 to $-1.31 \text{ kcal mol}^{-1}$) and the O_h complex ($\mathbf{1b}$: 8.63 – $11.41 \text{ kcal mol}^{-1}$) in the temperature range from 370 to -420 K , it is clear that $\mathbf{1c}$ would be preferred over $\mathbf{1b}$. In contrast, for $\mathbf{1a}$, the O_h complex $\{[\text{Co}_2(\mathbf{1})_2(\text{NO}_3)_2(\text{H}_2\text{O})_2] \cdot (\text{NO}_3)_2(\text{H}_2\text{O})_2\}_n$ has a large negative free energy (-1070 to $-1090 \text{ kcal mol}^{-1}$) in the same temperature range, and this provides a rationale for the fact that the O_h complex does not convert into the T_d geometry (Figure S5, Supporting Information). Thus, the calculated free-energy values for $\mathbf{1a}$, $\mathbf{1b}$, and $\mathbf{1c}$ are in excellent agreement with the experimental observations.

We measured the differential scanning calorimetry (DSC) thermograms of the gels (Figure S6, Supporting Information). To gain insight into the thermally promoted stability of $\mathbf{G1}$ and $\mathbf{G2}$, the transition temperatures ($T_{\text{sol-gel}}$) of $\mathbf{G1}$ and $\mathbf{G2}$ were measured by DSC. Compound $\mathbf{G1}$ exhibited a sharp phase transition at $145 \text{ }^\circ\text{C}$, whereas $\mathbf{G2}$ exhibited a sharp phase transition at $139 \text{ }^\circ\text{C}$ with an endothermic reaction. These endothermic thermograms are due to the transition of $\mathbf{G1}$ and $\mathbf{G2}$ into a solution phase, as observed in Figure S6 (Supporting Information). The $T_{\text{sol-gel}}$ of $\mathbf{G1}$ is higher than that of $\mathbf{G2}$ owing to strong gel formation with the octahedral structure.

Rheological studies of both $\mathbf{G1}$ and $\mathbf{G2}$ were performed to probe if there were rheological differences between these two gel types. We first used a dynamic strain sweep to determine the appropriate conditions for undertaking the subsequent examination of the gel by using the dynamic frequency sweep mode. As shown in Figure S7A (Supporting Information) in the linear viscoelastic region (LVR), the storage modulus (G') was higher than the loss modulus (G''). This is typical for the formation of a gel-phase material. For $\mathbf{G1}$ and $\mathbf{G2}$, the initial storage modulus (G') was higher than the loss modulus (G''), in keeping with the formation of a gel-phase material. We used the dynamic frequency sweep mode to study the composite gel after setting the strain amplitude at 0.1% (within the linear response region of the strain amplitude). The values of G' and G'' were almost constant with an increase in frequency from 0.1 to 100 rad s^{-1} (Figure S7B, Supporting Information). The value of G' was about 10 times larger than that for G'' over the whole range (10 – 600 rad s^{-1}), and this suggests that the gel is fairly tolerant to external forces. As observed on varying the dynamic strain sweep, the values of both G' and G'' for $\mathbf{G1}$ were almost the same to those for $\mathbf{G2}$. Furthermore, time-dependent oscillation measurements were also employed to monitor the gelation process for both $\mathbf{G1}$ and $\mathbf{G2}$ (Figure S7C, Supporting Information). The time sweep showed the rapid increase in G' and G'' in the initial stage of gelation, followed by a slower long-term approach to a final pseudoequilibrium plateau. At the end of the experiment, the value of G' was about six times higher than that of G'' .

On the basis of various response properties of the $\mathbf{G1}$ gels with Co^{2+} , we were able to model an AND logic gate by using the fact that this gate was operated through the addition of solid KBr and by mechanical grinding as inputs (1) and (2), respectively. As indicated in Figure 6A, the $\mathbf{G1}$ state remained unaltered (output = 0) upon the addition of one input [either (1) or (2)], whereas the simultaneous addition of the two inputs [both (1) and (2)] clearly altered $\mathbf{G1}$ to yield the blue color (output = 1), regardless of the order of the input. Similarly, we constructed an OR logic gate upon the addition of Br^- and Cl^- as two inputs (Figure 6B). The red color of $\mathbf{G1}$ changed to blue (output = 1) upon the addition of either Br^- or Cl^- . However, the red color was also altered upon the addition of both Br^- and Cl^- (corresponding to ionochromism). For this logic gate, it is clear that only one input is required to induce the color change.

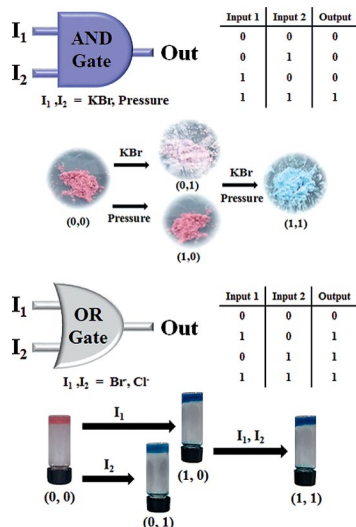


Figure 6. Gel-based supramolecular logic gates. (A) Photographs of the AND-type logic gate responses of xerogel **G1** (1: 2.0 wt.-%) with $\text{Co}(\text{NO}_3)_2$ (3 equiv.) toward KBr and pressure as input stimuli. (B) Photographs of the OR-type logic gate responses of **G1** (1: 2.0 wt.-%) with $\text{Co}(\text{NO}_3)_2$ (3.0 equiv.) toward Br^- and Cl^- as input stimuli.

Conclusions

We demonstrated that imidazole-based ligand **1** efficiently produces a coordination polymer gel by simple mixing with Co^{2+} ions. The coordination geometries of the imidazole-based gel with Co^{2+} were demonstrated to be anion-dependent. The octahedral coordination structure of the metal atom in **G1** was clearly confirmed by DFT calculations. If ligand **1** was present in less than 1 equiv. of CoCl_2 , the red octahedral structure formed as a sol. In contrast, blue **G2** was obtained if > 1 equiv. of CoCl_2 was present. The T_d structure in **G2** was the major form, and it coexisted with the O_h structures as minor complexes. The crystal of **1a** with $\text{Co}(\text{NO}_3)_2$ obtained for **G1** did not show a thermal response with a change in temperature owing to the thermal stability of the gel state. In contrast, the red single crystal of **1b** obtained in solution exhibited thermochromism and turned blue at higher temperature. The geometric change in **G1** from an octahedral structure to a tetrahedral structure upon the addition of either Br^- or Cl^- was indirectly demonstrated. The conversion of the red color of **G1** with octahedral structure into a blue color by introduction of Br^- or Cl^- appears to have involved anion exchange, which corresponds to the dissociation of two ligand molecules. No thermochromic effect was observed for **G2**, because **G2** with its T_d structure is thermodynamically more stable than octahedral **1b**. Furthermore, the ionochromic and the piezochromic effects observed for **G1** act as AND and OR logic gates. Hence, the concepts employed in the present study should point the way for the development of a range of new devices based on responsive soft materials such as **G1** described herein.

Experimental Section

X-ray Crystallographic Analysis: Crystal data for **1b** was collected with a Bruker SMART APEX II ULTRA diffractometer equipped with graphite-monochromated $\text{Mo-K}\alpha$ ($\lambda = 0.71073 \text{ \AA}$) radiation generated by a rotating anode and a CCD detector. The cell parameters for the compounds were obtained from a least-squares refinement of the spots (from 36 collected frames). Data collection, data reduction, and semiempirical absorption correction were performed by using the software package of APEX2.^[11] All of the calculations for the structure determination were performed by using the SHELXTL package.^[12] In all cases, the carbon atoms of one DMF molecule were disordered over two positions. CCDC-962778 (for **1b**) contains the supplementary crystallographic data for this paper. These data can be obtained free of charge from The Cambridge Crystallographic Data Centre via www.ccdc.cam.ac.uk/data_request/cif.

Preparation of a Single Crystal of 1a: A mixture of **1** (10 mg, 0.03 mmol) and $\text{Co}(\text{NO}_3)_2 \cdot 6\text{H}_2\text{O}$ (15 mg, 0.06 mmol) dissolved in DMF (5 mL) was placed in a 10 mL Pyrex glass tube. The tube was sealed and kept at 80°C for 24 h, which was followed by cooling to room temperature over 5 h. The single crystal obtained in DMF was used to determine the thermochromic effect, as shown Figure 4A.

Preparation of Single Crystal of 1b: A mixture of **1** (10 mg, 0.03 mmol) and $\text{CoCl}_2 \cdot 6\text{H}_2\text{O}$ (15 mg, 0.06 mmol) dissolved in DMF (5 mL) was placed in a 10 mL Pyrex glass tube. The tube was sealed and kept at 80°C for 24 h, which was followed by cooling to room temperature over 5 h. The single crystal obtained in DMF was used for structural analysis and to determine the thermochromic effect, as shown Figures 3b and B.

Preparation of Co^{2+} Supramolecular Gels: A solution of the cobalt salt (200 μL , 3.0 equiv. in DMF) was added to a solution of ligand **1** (2.0 wt.-% in DMF) in a vial. The metal coordination polymeric gel formed upon standing at ambient temperature. The gelation state of the material was evaluated by the criterion of “stable-to-inversion” performed in the test tube.

SEM Observations: Samples were taken with a field-emission scanning electron microscope (Philips XL30 S FEG). The acceleration voltage employed was 5–15 kV, and the emission current was 10 μA .

Photophysical Studies: UV/Vis absorption spectra were determined over the 200–800 nm range and were acquired both for the gel directly at room temperature and as a dispersion in DMF. UV/Vis absorption spectra of **G1** {[**1**] = 1 mM and Co^{2+} (0–3 equiv.)} and **G2** {[**1**] = 1 mM and Co^{2+} (0–3 equiv.)}.

DFT Calculations: The molecular geometries of **1a**, **1b**, and **1c** were optimized at the DFT level by employing the M06-2x functional with the 6-31G* basis set; calculations for **1a**, **1b**, and **1c** were performed at the M06-2x/3-21G* level because of their high computation speed concerns. All calculations were performed with the suite of Gaussian 09 programs.^[10] Binding free energies of single crystals **1a**, **1b**, and **1c** were calculated at a constant pressure of 101.3 kPa with temperature.

DSC Measurements: DSC was performed with a Seiko DSC6100 high-sensitivity differential scanning calorimeter equipped with a liquid-nitrogen cooling unit. Samples of the Co^{2+} coordination polymer gels were hermetically sealed in a silver pan and measured against a pan containing alumina as the reference. The thermograms were recorded at a heating rate of $0.5^\circ\text{C min}^{-1}$.

Rheological Measurements: These were performed with freshly prepared gels by using a controlled stress rheometer (AR-2000ex, TA Instruments, Ltd., New Castle, DE, USA). Parallel cone geometry of 40 mm diameter was employed throughout. Dynamic oscillatory work kept a frequency of 1 rad s^{-1} . The following tests were performed: increasing amplitude of oscillation up to 200% apparent strain on shear, time and frequency sweeps at $25 \text{ }^\circ\text{C}$ (60 min and from $0.1\text{--}100 \text{ rad s}^{-1}$, respectively).

Logic-Gates Measurements: The color changes of **G1** were observed upon the addition of either Br^- or Cl^- . In addition, the color changes of dry **G1** with solid KBr were observed by pressure (56 atm) at room temperature.

Supporting Information (see footnote on the first page of this article): X-ray crystallographic data, experimental details, and characterization data.

Acknowledgments

This work was supported by the Ministry of Education, Science and Technology, Korea through the National Research Foundation of Korea (NRF) (2012002547 and 2012R1A4A1027750). In addition, this work was partially supported by a grant from the Next-Generation BioGreen 21 Program [System & Synthetic Agrobiotech Center (SSAC), grant PJ009041], Rural Development Administration, Korea.

- [1] a) F. Fages, *Angew. Chem. Int. Ed.* **2006**, *45*, 1680–1682; *Angew. Chem.* **2006**, *118*, 1710–1712; b) H.-J. Kim, J.-H. Lee, M. Lee, *Angew. Chem. Int. Ed.* **2005**, *44*, 5810–5814; *Angew. Chem.* **2005**, *117*, 5960–5964; c) B. Xing, M.-F. Choi, B. Xu, *Chem. Eur. J.* **2002**, *8*, 5028–5032; d) W. Weng, J. B. Beck, A. M. Jamieson, S. J. Rowan, *J. Am. Chem. Soc.* **2006**, *128*, 11663–11672; e) J. H. Jung, J. H. Lee, J. R. Silverman, G. John, *Chem. Soc. Rev.* **2013**, *42*, 924–936; f) L. E. Kreno, K. Leong, O. K. Farha, M. Allendorf, R. P. Van Duyne, J. T. Hupp, *Chem. Rev.* **2012**, *112*, 1105–1125; g) S. Dong, Y. Luo, X. Yan, B. Zheng, X. Ding, Y. Yu, Z. Ma, Q. Zhao, F. Huang, *Angew. Chem. Int. Ed.* **2011**, *50*, 1905–1909; *Angew. Chem.* **2011**, *123*, 1945–1949; h) M. Zhang, D. Xu, X. Yan, J. Chen, S. Dong, B. Zheng, F. Huang, *Angew. Chem. Int. Ed.* **2012**, *51*, 7011–7015; *Angew. Chem.* **2012**, *124*, 7117–7121; i) S. Dong, B. Zheng, D. Xu, X. Yan, M. Zhang, F. Huang, *Adv. Mater.* **2012**, *24*, 3191–3195; j) X. Yan, D. Xu, X. Chi, J. Chen, S. Dong, X. Ding, Y. Yu, F. Huang, *Adv. Mater.* **2012**, *24*, 362–369; k) G. Yu, X. Yan, C. Hana, F. Huang, *Chem. Soc. Rev.* **2013**, *42*, 6697–6722.
- [2] a) J. He, J.-X. Zhang, C.-K. Tsang, Z. Xu, Y.-G. Yin, D. Li, S.-W. Ng, *Inorg. Chem.* **2008**, *47*, 7948–7950; b) T. H. Kim, Y. W. Shin, J. H. Jung, J. S. Kim, J. Kim, *Angew. Chem. Int. Ed.* **2008**, *47*, 685–688; *Angew. Chem.* **2008**, *120*, 697–700; c) Q. Zhu, T. Sheng, C. Tan, S. Hu, R. Fu, X. Wu, *Inorg. Chem.* **2011**, *50*, 7618–7624; d) Y. Funasako, T. Mochida, *Chem. Commun.* **2013**, *49*, 4688–4690; e) A. M. Goforth, M. A. Tershansy, M. D. Smith, L. Peterson Jr., J. G. Kelley, W. I. DeBenedetti, H. Loye, *J. Am. Chem. Soc.* **2011**, *133*, 603–612.
- [3] a) G. Mehlana, S. A. Bourne, G. Ramon, L. Ohrstrom, *Cryst. Growth Des.* **2013**, *13*, 633–644; b) S. Gadzuric, M. Vranes, S. Dozic, *Sol. Energy Mater. Sol. Cells* **2012**, *105*, 309–316; c) C. Shen, T. Sheng, Q. Zhu, S. Hu, X. Wu, *CrystEngComm* **2012**, *14*, 3189–3198; d) N. Carmona, V. Bouzas, F. Jimenez, M. Plaza, L. Perez, M. A. Garcia, M. A. Villegas, J. Llopis, *Sens. Actuators B* **2010**, *145*, 139–145.
- [4] K. Kuroiwa, T. Shibata, A. Takada, N. Nemoto, N. Kimizuka, *J. Am. Chem. Soc.* **2004**, *126*, 2016–2021.
- [5] O. Roubeau, A. Colin, V. Schmitt, R. Clerac, *Angew. Chem. Int. Ed.* **2004**, *43*, 3283–3286; *Angew. Chem.* **2004**, *116*, 3345–3348.
- [6] H. Lee, S. H. Jung, W. S. Han, J. H. Moon, S. Kang, J. Y. Lee, J. H. Jung, S. Shinkai, *Chem. Eur. J.* **2011**, *17*, 2823.
- [7] A. Rit, T. Pape, A. Hepp, F. E. Hahn, *Organometallics* **2011**, *30*, 334–347.
- [8] a) T. Nakashima, K. Miyamura, T. Sakai, T. Kawai, *Chem. Eur. J.* **2009**, *15*, 1977–1984; b) I. Georgieva, A. J. A. Aquino, N. Trendafilova, P. S. Santos, H. Lischka, *Inorg. Chem.* **2010**, *49*, 1634–1646.
- [9] a) T. Han, Y. Zhang, X. Feng, Z. Lin, B. Tong, J. Shi, J. Zhi, Y. Dong, *Chem. Commun.* **2013**, *49*, 7049–7051; b) Y. Dong, B. Xu, J. Zhang, X. Tan, L. Wang, J. Chen, H. Lv, S. Wen, B. Li, L. Ye, B. Zou, W. Tian, *Angew. Chem. Int. Ed.* **2012**, *51*, 10782–10785; *Angew. Chem.* **2012**, *124*, 10940–10943.
- [10] M. J. Frisch, G. W. Trucks, H. B. Schlegel, G. E. Scuseria, M. A. Robb, J. R. Cheeseman, G. Scalmani, V. Barone, B. Mennucci, G. A. Petersson, H. Nakatsuji, M. Caricato, X. Li, H. P. Hratchian, A. F. Izmaylov, J. Bloino, G. Zheng, J. L. Sonnenberg, M. Hada, M. Ehara, K. Toyota, R. Fukuda, J. Hasegawa, M. Ishida, T. Nakajima, Y. Honda, O. Kitao, H. Nakai, T. Vreven, J. A. Montgomery Jr., J. E. Peralta, F. Ogliaro, M. Bearpark, J. J. Heyd, E. Brothers, K. N. Kudin, V. N. Staroverov, R. Kobayashi, J. Normand, K. Raghavachari, A. Rendell, J. C. Burant, S. S. Iyengar, J. Tomasi, M. Cossi, N. Rega, J. M. Millam, M. Klene, J. E. Knox, J. B. Cross, V. Bakken, C. Adamo, J. Jaramillo, R. Gomperts, R. E. Stratmann, O. Yazyev, A. J. Austin, R. Cammi, C. Pomelli, J. W. Ochterski, R. L. Martin, K. Morokuma, V. G. Zakrzewski, G. A. Voth, P. Salvador, J. J. Dannenberg, S. Dapprich, A. D. Daniels, Ö. Farkas, J. B. Foresman, J. V. Ortiz, J. Cioslowski, D. J. Fox, *Gaussian 09*, Revision A.1, Gaussian, Inc., Wallingford, CT, **2009**.
- [11] *APEX2: Data Collection and Processing Software*, version 2009.1–0, Bruker AXS, Inc., Madison, WI, **2008**.
- [12] G. M. Sheldrick, *Acta Crystallogr., Sect. A* **2008**, *64*, 112–122.

Received: March 8, 2014

Published Online: April 8, 2014